



An overview of events of high sea waves at the mouth of Guanabara Bay

VICTOR A. GODOI^{1,2*}, CARLOS E. PARENTE RIBEIRO¹ & AUDÁLIO R. TORRES JR.³

¹Federal University of Rio de Janeiro, Ocean Engineering Program, COPPE, Cidade Universitária, Ilha do Fundão, CEP: 21945-970, Rio de Janeiro, RJ, Brazil. *Corresponding author: victorgodoirj@gmail.com

²University of Waikato, Faculty of Science and Engineering, Department of Earth and Ocean Sciences, Coastal Marine Group, Knighton Rd, Hamilton 3240, Waikato, New Zealand.

³Federal University of Rio de Janeiro, Institute of Geosciences, Department of Meteorology. Av. Brigadeiro Trompowski, s/n°, Cidade Universitária, Ilha do Fundão, CEP: 21949-900, Rio de Janeiro, RJ, Brazil.

Abstract. An overview of five events of high sea waves at the mouth of Guanabara Bay has been presented in this study. These events happened in the years of 1988, 1997, 2008, 2009 and 2010. In order to assess the order of magnitude of mean wave parameters during such events, the WAVEWATCH III model was implemented forced by wind fields from the NCEP-NCAR Reanalysis I project. A validation of the simulations was carried out by comparing their results to the nearest grid point results of the NOAA global wave hindcast, since wave measurements are not available in the study region. The 2010 event presented the highest value of significant wave height (4.68-m) and the lowest value was found in the 2008 event (1.86-m). The hindcasts presented mean values of 3.54-m for significant wave height (SWH), 12.84-s for peak wave period (TP) and 163.9° for peak wave direction (DP) in times of maxims SWHs. Monthly and seasonal climatologies were generated for mean wave parameters close to the region of study from the same global wave hindcast used to validate the results of the present work. In the first, the highest value of SWH was found in September, suggesting a relationship with the high frequency of cold fronts that move along the Brazilian shore during this month. In the second, winter presented the highest values for SWH and TP, as usual in the literature.

Key words: Guanabara bay, events of high sea waves, wave modelling, regional wave hindcast

Resumo. Uma visão geral de eventos de ressacas marítimas na boca da Baía de Guanabara. Uma visão geral de cinco eventos de ressacas marítimas na boca da Baía de Guanabara é apresentada neste estudo. Esses eventos ocorreram nos anos de 1988, 1997, 2008, 2009 e 2010. A fim de avaliar a ordem de grandeza dos parâmetros médios de onda durante tais eventos, o modelo WAVEWATCH III foi implementado usando os campos de vento do projeto *Reanalysis* I do NCEP-NCAR como condições de contorno. Uma validação das simulações foi realizada a partir da comparação com os resultados do ponto de grade mais próximo da simulação global de ondas conduzida pela NOAA, uma vez que medições de onda não estão disponíveis na região de estudo. O maior valor de altura significativa de onda (4,68-m) ocorreu no evento de 2010 e o menor valor (1,86-m) no evento de 2008. Os valores médios encontrados nas simulações durante os horários de alturas significativas máximas de onda foram 3,54-m para altura significativa de onda (SWH), 12,84-s para o período de pico (TP) e 163,9° para a direção de pico (DP). Climatologias mensal e sazonal foram geradas para os parâmetros médios de onda próximo à região de estudo a partir da mesma simulação global usada para validar os resultados do presente trabalho. Na primeira, o maior valor de SWH foi encontrado em setembro, sugerindo uma relação com a alta frequência de frentes frias que se movem ao longo da costa brasileira durante este mês. Na segunda, o inverno apresentou os maiores valores para SWH e TP, como de costume na literatura.

Palavras chave: Baía de Guanabara, eventos de ressacas marítimas, modelagem de onda, simulação pretérita regional de onda

Introduction

Several studies have been conducted in order to characterize events of high sea waves (EHSW) in many regions worldwide (e.g. Khandekar & Swail, 1995; Holliday *et al.*, 2006; Stephens & Gorman, 2006; Ledden *et al.*, 2009). On the other hand, only a few works regarding this topic were accomplished for the southwestern Atlantic Ocean up to now (e.g. Innocentini & Caetano Neto, 1996; Innocentini *et al.*, 2003; Rocha *et al.* 2004; Dragani *et al.*, 2013). Guanabara Bay (GB), Rio de Janeiro state – Brazil, receives EHSW on a relatively low frequency (Kjerfve *et al.*, 1997), resulting in little attention to be devoted to them. However, such events have brought

serious damages in different places inside the estuary.

Guanabara Bay (Fig. 1) is among the most valuable estuaries of the country due to its economic and social importance. It is centered on latitude $22^{\circ}50'S$ and longitude $43^{\circ}10'W$ (Kjerfve *et al.*, 1997). Rio de Janeiro city, the second largest industrial complex and the second largest demographic center of the country, is situated around GB, which in turns still comprises about 6000 industries, 16 maritime oil terminals, 2 commercial harbors, 2 oil refineries and 13 shipyards (CIDS, 2000). Furthermore, many people use GB to commute mainly between Rio de Janeiro and Niterói cities.

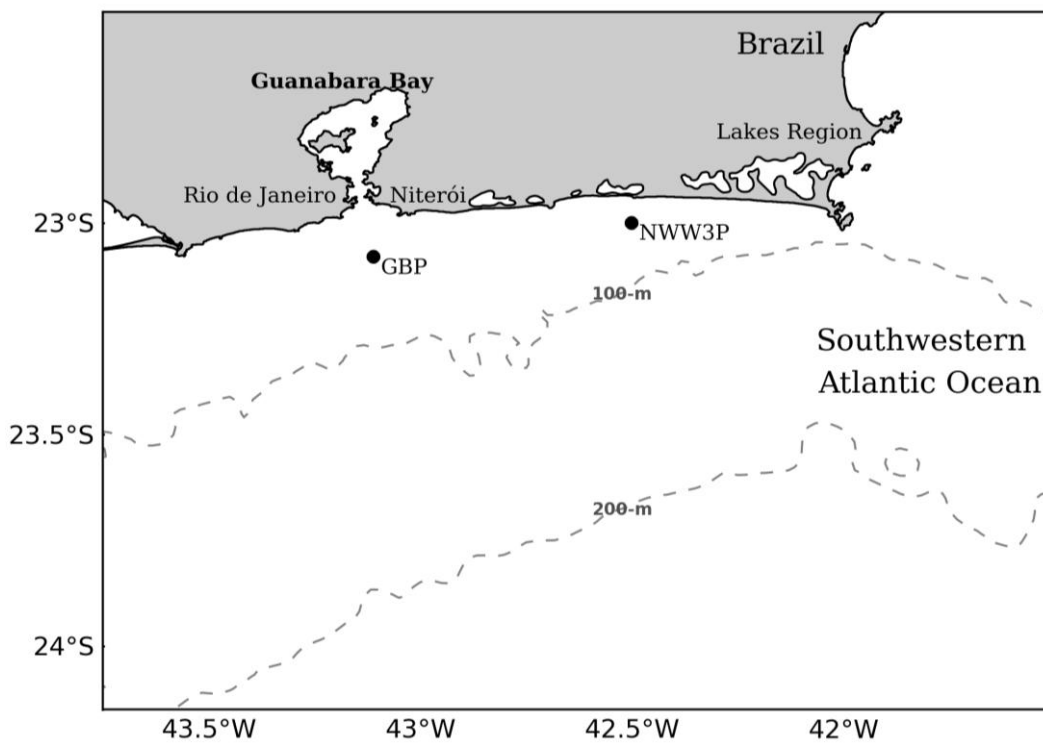


Figure 1. Study area. Wave models output grid points are pointed out with black circles. GBP: Guanabara Bay output grid point – location where the time series of mean wave parameters were computed in the simulations performed in this work; NWW3P: NOAA wave hindcast output grid point – this is the nearest grid point to the mouth of Guanabara Bay in the global wave hindcast produced by the NOAA.

Historic EHSW that took place at GB brought significant damages to its coastal structures and surrounding areas. One person died and a drainage pipe with 8000-kg disappeared in August 1988 (Innocentini & Caetano Neto, 1996). Many boats were destroyed by the waves in the Glória marina in May 1997 and some waves overran Santos Dumont airport

runways in April 2010. The people transportation maritime service had to be interrupted owing to the wave heights during some events, such as April 2008 and April 2010. Innocentini & Caetano Neto (1996) simulated the event of August 1988 by coupling a limited-area atmospheric model and a second-generation wave model. The authors obtained

significant wave heights (SWHs) of about 4-m very close to GB. Candella *et al.* (1999) simulated the event of May 1997 by using the WAM model and obtained SWHs exceeding 2.75-m at approximately 90-km from the GB entrance. Therefore, the knowledge about the order of magnitude of waves during EHSW is of great importance to avoid damages inside GB and its surroundings.

Unfortunately, wave parameters have not been recorded by oceanographic instruments in the region. It has been an obstacle to study EHSW and to assess their impacts on coastal structures. Additionally, the lack of measurements throughout the years limits the generation of a wave climatology of the region. Numerical modeling has been the most common alternative to remedy the shortage of wave measurements. A lot of wave models (e.g. WAM, WAVEWATCH III, REF/DIF, SWAN) have been developed and improved lately to achieve different purposes. Some of them focus on the wave generation and propagation processes, while others focus on the wave modification processes when waves reach intermediate and shallow waters.

Given the need to comprehend the order of magnitude of mean wave parameters during EHSW at GB, five noteworthy events were hindcasted in the present study. Simulated time series of significant wave height (SWH), peak wave period (TP) and peak wave direction (DP) were assessed at the mouth of GB during events that happened in the years of 1988, 1997, 2008, 2009 and 2010. The hindcasts were carried out by using the WAVEWATCH III version 3.14 (Tolman, 2009) forced by wind fields sourced from the Reanalysis I project (Kalnay *et al.*, 1996) of the National Centers for Environmental Prediction – National Center for Atmospheric Research (NCEP-NCAR). Atmospheric parameters acquired from the NCEP-NCAR Reanalysis I project helped interpreting the occurrence of such events. A global wave hindcast (NWW3), produced by the National Oceanic and Atmospheric Administration (NOAA), was utilized to validate the results of the EHSW hindcasts and also to assess the simulated wave climate at a point near the region of study.

This paper is organized as follows. A brief explanation about the datasets used in the meteorological analysis and in the numerical modeling is made in section 2. Section 3 addresses the climatology of cyclogenesis in South America (SA). Section 4 describes the selection of EHSW, and the settings of numerical modeling are described in

section 5. The results are discussed in section 6. Finally, the conclusions are presented in section 7.

Datasets

Three types of datasets have been used in the development of the present study: atmospheric, bathymetric and modeled wave datasets. All of them have been widely adopted by the international community due to their reliability. The datasets are outlined below.

Atmospheric data

The atmospheric data were sourced from the NCEP-NCAR Reanalysis I project, that aims at producing global atmospheric fields analyses. In order to do so, data from many sources, such as rawinsondes, ships, satellites and meteorological stations are assessed by a quality control system and post processed by using numerical modeling with data assimilation. Thus, three low level parameters were collected from that project in the region limited by the spatial range of 70°S-0° and 80°W-0°, zonal and meridional components of the wind at 10-m (u10, v10) and the mean sea level pressure (MSLP). The spatial resolution of MSLP fields is 2.5° x 2.5° and of u10 and v10 fields is 1.8750° x 1.9047°. The three parameters have temporal resolution of 6-hours. Relative vorticity fields at 10-m were calculated from u10 and v10 in order to compute horizontally-averaged relative vorticity time series. These time series were used to identify the presence of atmospheric cyclonic systems during the occurrence of the EHSW addressed here. The wind components at 10-m were also employed as boundary conditions in the wave hindcasts. Mean sea level pressure fields were used to associate the EHSW with atmospheric systems.

Bathymetric data

The bathymetric data were taken from two different sources, the National Geophysical Data Center (NGDC-NOAA) ETOPO1 database (Amante & Eakins, 2009) and the Brazilian navy nautical charts. The first database is composed by the results of the 1 arc-minute global relief model ETOPO1, which provides land topography and ocean bathymetry at four different spatial resolutions (1', 2', 4' and 10') to the South Atlantic Ocean. This database has been developed to support tsunami forecasting and ocean modeling. The Brazilian navy nautical charts, produced to assist the navigation, are made from bathymetric measurements acquired with specific instruments and have irregularly spaced bathymetry,

with spatial resolutions higher than 1 minute for coastal areas. Then, bathymetric data were interpolated in order to create numerical grids to be used in the wave hindcasts, resulting in the spatial

resolutions depicted in the forth column of Table I. In the same table are also presented the ranges of the grid domains.

Table I. Grids domains used in the wave hindcasts.

| Grids | Latitude range (deg.) | Longitude range (deg.) | Spatial resolution (min.) |
|--------|-----------------------|------------------------|---------------------------|
| Grid 1 | -68 to -2 | -78 to -15 | 27 |
| Grid 2 | -45 to -10 | -60 to -20 | 9 |
| Grid 3 | -30 to -18 | -50 to -35 | 3 |
| Grid 4 | -25 to -22 | -46 to -42 | 1 |
| Grid 5 | -23.09 to -22.69 | -43.32 to 43.00 | 0.25 |

Global wave hindcast

A 13-year (1997-2009) global wave hindcast (hereinafter NWW3) was carried out by the NCEP-NOAA employing the WAVEWATCH III (Tolman, 2009) model forced by wind fields and air-sea temperature differences derived from the Global Forecast System (GFS). The NWW3 results comprise mean wave parameters fields (SWH, DP and TP) with a spatial resolution of $1.25^\circ \times 1.0^\circ$ at 3-h intervals. These results are freely available for downloading at <http://polar.ncep.noaa.gov/waves>. The NWW3 results were utilized for two purposes, validate the results of the EHSW simulations and generate monthly and seasonal climatologies for mean wave parameters near the region of study. The nearest NWW3 grid point to the mouth of GB (NWW3P in Fig. 1), located at $42.5^\circ\text{W} \times 23^\circ\text{S}$, was chosen to accomplish both tasks.

A brief description of the South America cyclogenesis climatology

Cyclones are the weather systems that trigger the kind of EHSW investigated in the present paper. Therefore, places of origin and frequencies of occurrence of these systems are briefly described in this section. There is a lack of consensus regarding the intensity and the seasonal preference of cyclogenesis, as well as on the number of cyclogenesis during *El Niño* years.

Streten & Troup (1973) have already noticed a pattern of cyclonic formation in the east of SA by analyzing satellite data mosaic sequences over the Southern Hemisphere. Two preferential regions of cyclogenesis have been found in SA, one in the east of Argentina ($42.5^\circ\text{S} \times 62.5^\circ\text{W}$) and another in the east of Uruguay ($31.5^\circ\text{S} \times 55^\circ\text{W}$) (Gan & Rao, 1991;

Sinclair, 1995; Rocha *et al.*, 2004, Reboita *et al.*, 2010). Sinclair (1995) investigated life cycle characteristics of cyclones in the Southern Hemisphere. In that study, the author indicates the existence of a third cyclogenetic region in southern Brazil, that would be a weaker genesis maximum when compared to the first two mentioned regions. On the contrary, Seluchi (1995) mentions that the region between 20 and 35°S over the eastern part of SA is one of the strongest cyclogenetic regions of the Southern Hemisphere. The author analyzed the mean synoptic conditions associated with the eastern SA cyclogenesis and proposed objective methods to forecast them. A more recent study, developed by Reboita *et al.* (2010), addresses the climatology of cyclogenesis over the Southern Atlantic Ocean (SAO) from 1990 to 1999. The authors had run the Regional Climate Model (RegCM3) and identified three cyclogenetic regions in the west sector of SAO. The third most active cyclogenetic region was located over the south/southeastern coast of Brazil, in agreement with Sinclair (1995).

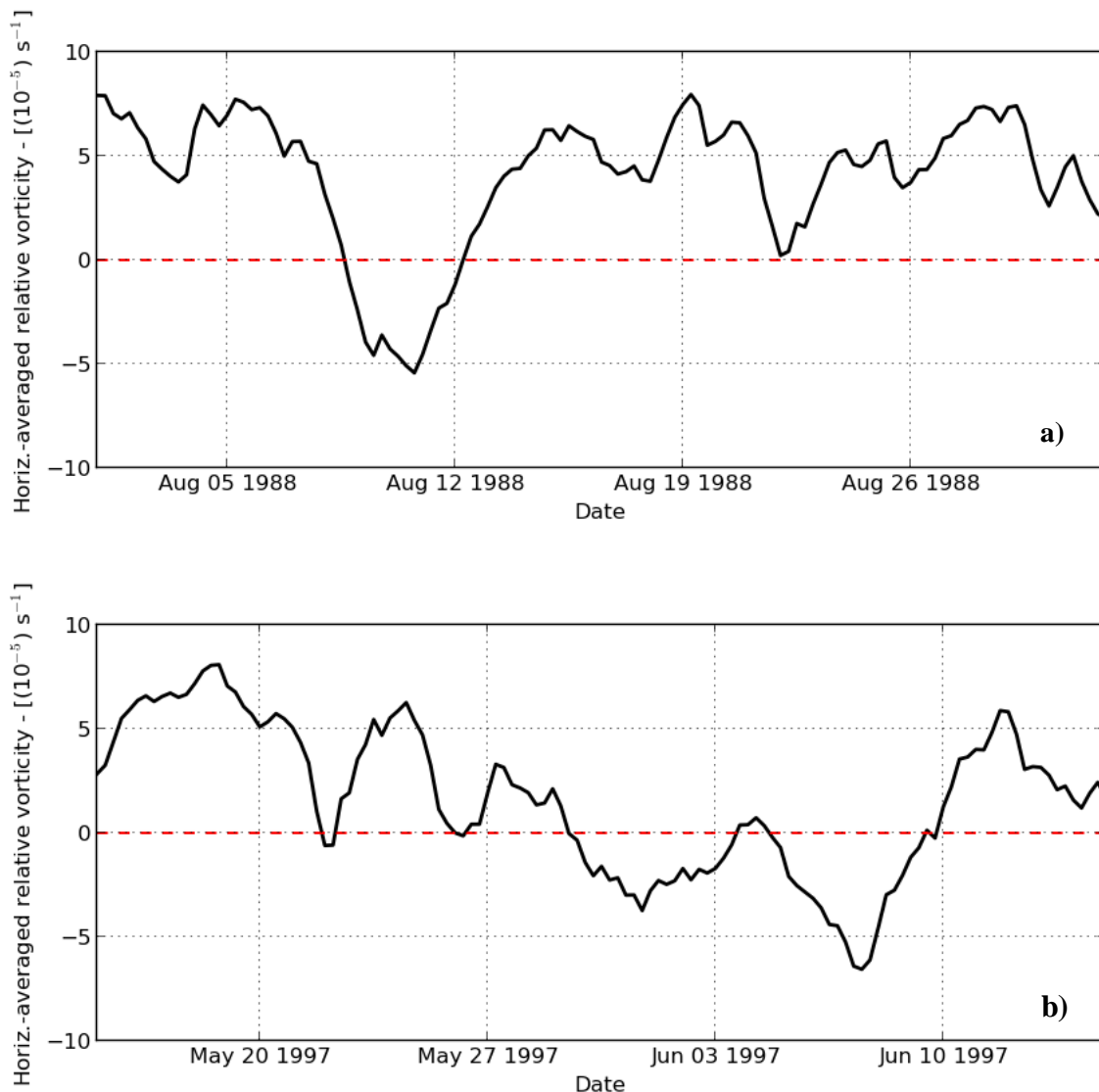
Based on satellite cloud imagery and synoptic charts, Satyamurty *et al.* (1990) studied the frequency of cyclones and cyclonic development, as well as preferred areas and seasons of their generation over SA from 1980 to 1986. According to the study, there are more cyclogenesis in summer than in winter. Another important conclusion is that there were about 25% more vortex formations in 1983 (*El Niño* year) than in neutral years. Gan & Rao (1991) used different datasets in order to verify the seasonal preference of surface cyclogenesis over SA. In contrast to Satyamurty *et al.* (1990), Gan & Rao (1991) observed that the number of cyclones increases during winter season, but the highest frequency of occurrence

happens in the month of May. In addition, the authors state the number of cyclogenesis is higher during *El Niño* years. On the other hand, Beu & Ambrizzi (2006) concluded that years of *El Niño* are similar to neutral years in terms of number of cyclones by analyzing 30-year NCEP-NCAR MSLP data (1969-1999). Moreover, they realized the number of cyclones increased in spring season during *La Niña* events.

Selection of events of high sea waves

Events of high sea waves at the mouth of GB have not been commonly reported by scientific papers. On the contrary, the Brazilian news media has shown how damaging those events have been. Examples of remarkable EHSW occurred in the following dates: August 11, 1988; May 31, 1997; April 24, 2008; October 02, 2009 and April 08, 2010. These events were chosen to be assessed in this study and they will be named according to their years of occurrence hereinafter. In order to corroborate the dates of occurrence provided by the news media, since there

is no scientific evidence that those EHSW occurred indeed, it was decided to assess time series that could provide with this information. Then, time series of horizontally-averaged relative vorticity were computed in the region limited by the spatial ranges of 20° to 40° S and 55° to 20° W. This task was accomplished by using u_{10} and v_{10} wind fields sourced from NCEP-NCAR Reanalysis I project. The aforementioned spatial ranges were defined because they encompass the main area of displacement of cyclones (MADC), avoiding contamination from other systems. The permanence of cyclonic systems in MADC may favor the formation of a wave fetch toward the study area and, in some occasions, may result in the occurrence of EHSW. Spatial and temporal dominances of cyclonic systems in MADC during the selected EHSW can be observed in Figure 2 through negative values of horizontally-averaged relative vorticity.



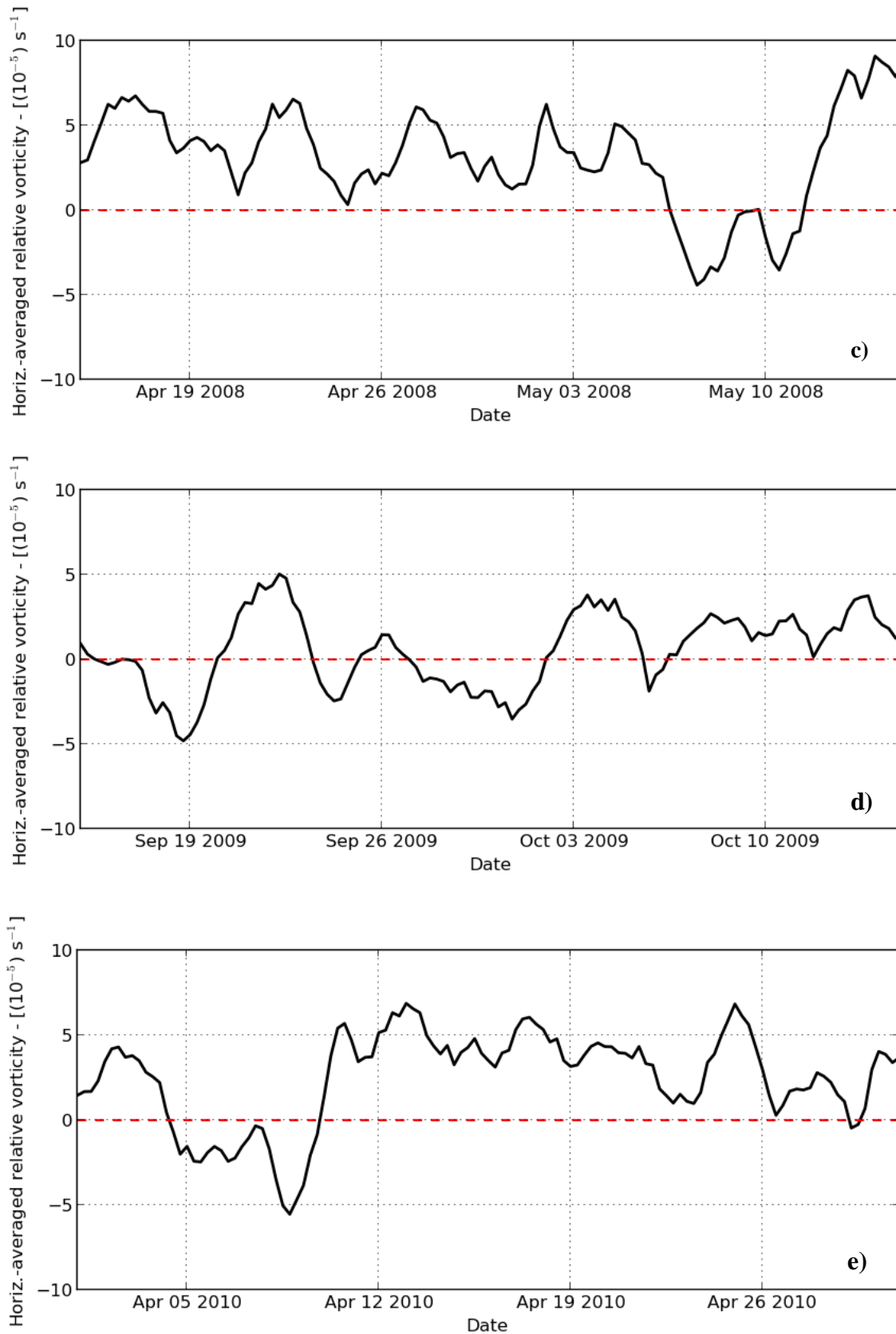


Figure 2. Time series of horizontally-averaged relative vorticity computed in the region limited by the spatial ranges of 20° to 40°S and 55° to 20°W in the years of (a) 1988; (b) 1997; (c) 2008; (d) 2009 and (e) 2010.

In Figure 2, negative peaks are in accordance with the dates of EHSW, except in the 2008 event (Fig. 2c). In fact, the MADC does not encompass the trajectory of the 2008 cyclone during the period presented because it had propagated south of the area. Additionally, the cyclone remained almost steady southeast of the MADC while had generated waves toward GB and it had already dissipated at the moment of occurrence of high waves. This indicates that waves took a considerable time to reach the mouth of GB owing to the distance between the wave generation zone and the study area. In the 2009 event, the negative peak disappears some hours before the event takes place (Fig. 2d), which suggests the cyclone was already out of the MADC when the waves reached the mouth of GB.

Wave model hindcasts

The WAVEWATCH III v. 3.14 (Tolman, 2009) was implemented to hindcast particular EHSW at the mouth of GB. This model has been extensively used for many regions of the world with a broad range of applications (e.g. Alves *et al.*, 2009; Stopa *et al.*, 2011; Chawla *et al.*, 2013). This is a third generation wave model that solves the wave action density spectrum as a function of wavenumber and direction. Parameterizations of physical processes include wave growth and decay by wind stress, nonlinear resonant interactions, bottom friction, dissipation by white-capping, surf-breaking and scattering by wave-bottom interactions. In shallow waters, the governing equation still includes refraction and straining of the wave field due to temporal and spatial variations of the mean water depth and of the mean current. Additional information about the model can be found in Tolman (2009).

Input and dissipation terms were computed by the Tolman & Chalikov (1996) formulation and nonlinear wave-wave interactions were modeled by using the discrete interaction approximation (DIA, Hasselmann *et al.*, 1985). The bottom friction was represented by the Joint North Sea Wave Project (JONSWAP) parameterization (Hasselmann *et al.*, 1973). The formulation proposed by Cavaleri & Malanotte-Rizzoli (1981) was used to improve the initial wave growth behavior from calm conditions. Tidal oscillations were not taken into account.

The evolution of the directional wave spectrum was computed by using 25 logarithmically-spaced frequencies, starting at 0.04118-Hz with increment factor of 1.1, and 24 directions. The local

spectrum was calculated using the local wind speed and direction during initial conditions, using the spatial grid size as fetch. Five spherical grids were one-way nested (Fig. 3) according to the spatial ranges and resolutions presented in Table I. Wind fields, derived from the NCEP-NCAR Reanalysis I project, were employed as surface forcing in all grid domains at 6-h intervals (UTC). Cold start runs, with flat sea surface, were then performed. Time series of significant wave height, peak wave period and peak wave direction were evaluated at the point (represented by the acronym GBP in Fig. 1) located at 14.11-km (43.11°W x 23.08°S) from the GB entrance, on a depth of 45-m. This location was established to avoid misinterpretation of the peak wave direction due to obstacles, such as islands or extreme shallow waters.

The model was then run for a period of 15 days for each simulation, discarding the first six days because of the model spin-up. For the existence of a balanced and consistent numerical integration scheme, mean wave parameters were output at intervals of 1.2-h. This consistency follows the assumption of proportionality among the overall time step and input and output time intervals of the model, as proposed by Tolman (2009). Unfortunately, the lack of wave observations nearby the output point has not allowed the direct verification of the hindcasts in GBP. However, a validation of the EHSW simulations was carried out by comparing the obtained results of SWH, TP and DP to the NWW3 results at the point 42.5°W x 23°S (NWW3P). In order to do so, the NWW3 results were linearly interpolated to match the output time intervals of the EHSW results and then, a basic wave statistics was performed. The mean, standard deviation, bias (bias = EHSW modeled results – NWW3 results), root-mean-square error (RMSE), scatter index (SI = RMSE / mean) and the Pearson's correlation coefficient (R) were computed for the 1997, 2008 and 2009 events, since the other events are not included in the NWW3 results.

Results and discussion

In the period between the years of 1988 and 2010, five EHSW at the mouth of GB can be highlighted due to their significant impacts. Mean sea level pressure fields and hindcasted time series of mean wave parameters (SWH, TP and DP) in GBP are shown as follows for each event (Fig. 4). The intent of illustrating MSLP fields is to depict the cyclonic

systems that triggered the EHSW. They are shown in the following dates: August 10, 1988; May 31, 1997; April 22, 2008; September 30, 2009 and April 08,

2010; which do not necessarily match the instants of maximum significant wave height.

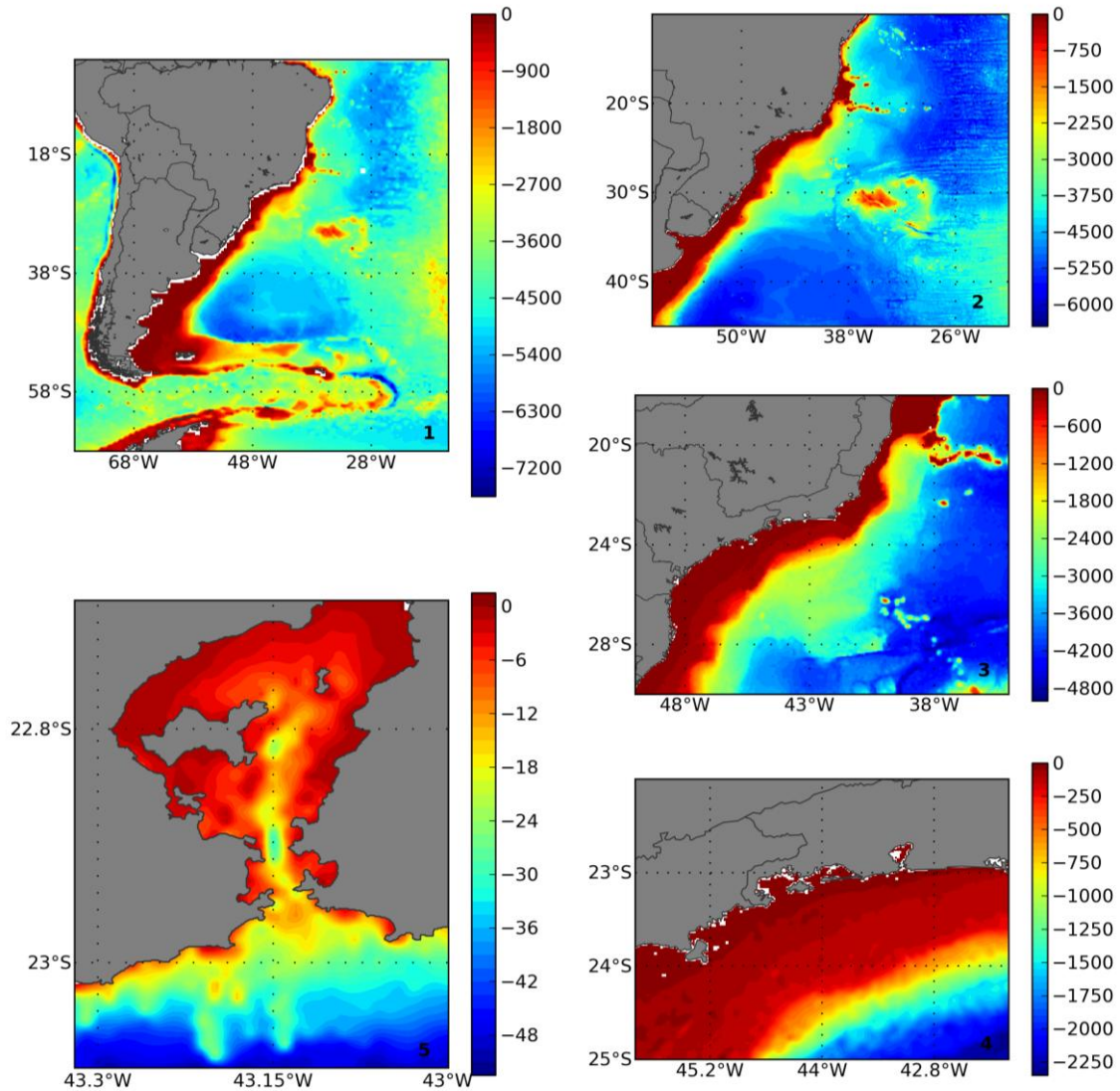


Figure 3. Numerical grids of the wave modeling. The numbers 1 to 5 refer to the numbers of the grid domains, as exposed in Table I. Colors represent the bathymetry in meters.

The cyclone responsible for the 1988 event (Fig. 4a – left panel) had been formed over the east of Uruguay (31.5°S x 55°W) and moved to ESE. Its propagation was faster during the first two days. This atmospheric system generated the second highest modeled SWH among those addressed here, reaching 4.37-m (Fig. 4a – right panel). The results of the 1988 event are in agreement with those obtained by Innocentini & Caetano Neto (1996) for SWH, that obtained values of

about 4-m close to the coast. The 1997 cyclone (Fig. 4b – left panel) had been formed over the southern coast of Brazil, the region mentioned by Sinclair (1995) and Reboita *et al.* (2010) as the third region of greatest cyclogenetic activity in SA. This cyclone moved eastward for few hours and then, turned to SE until remains almost steady very close to GB for two days. At that position, the cyclone deepened and generated waves up to 3.85-m

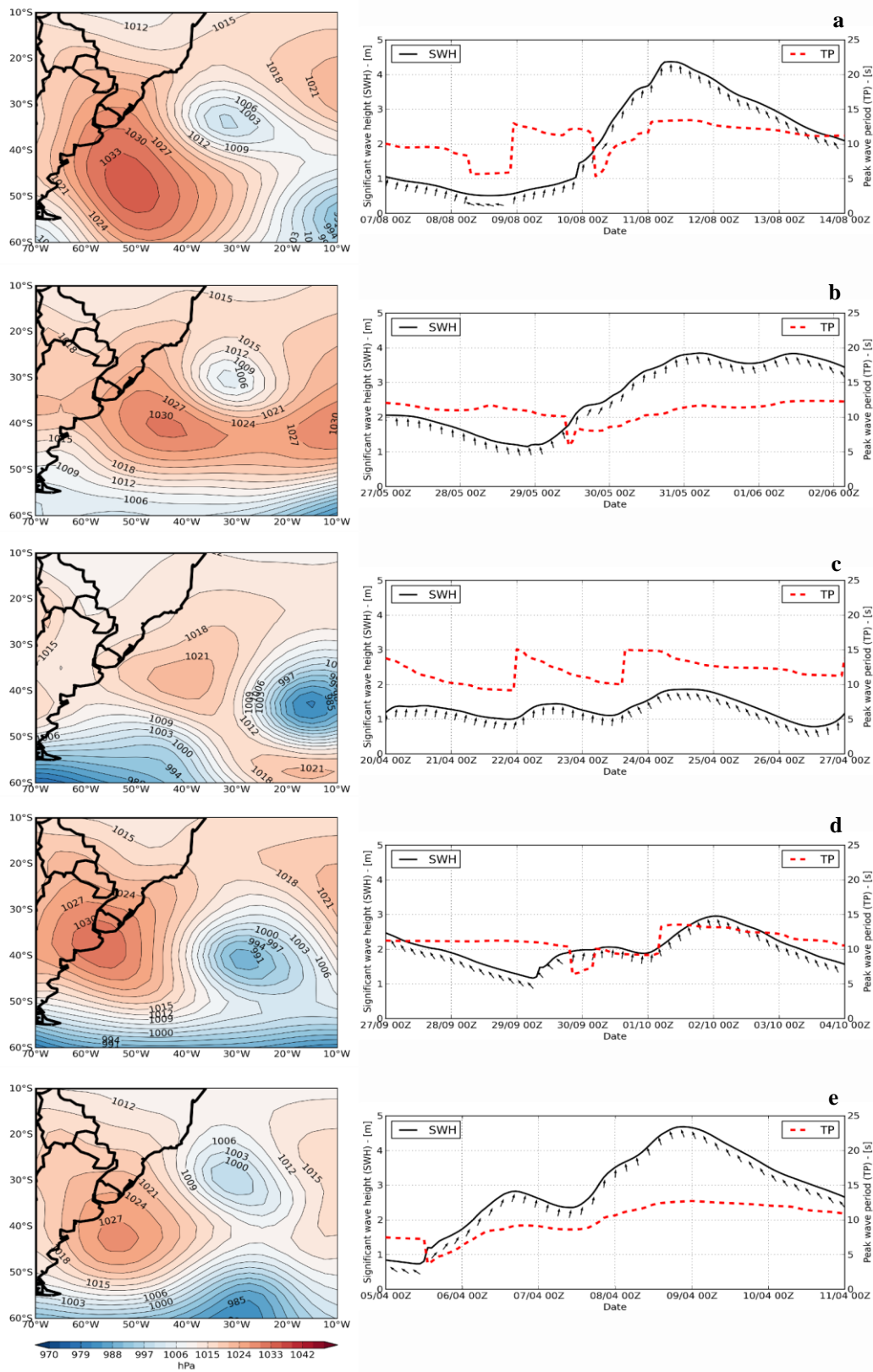


Figure 4. Mean sea level pressure fields (left panels) and hindcasted time series of mean wave parameters (right panels) for the events of (a) 1988; (b) 1997; (c) 2008; (d) 2009 and (e) 2010. In right panels, solid lines represent significant wave heights; dashed lines represent peak wave periods; and arrows represent peak wave directions.”

(Fig. 4b – right panel). Candella *et al.* (1999) carried out a wave simulation for this event by employing the WAM model and obtained approximately 2.80-m for the maximum SWH at the GB nearest grid point (23°S x 42.5°W). This value is 37% lower than the one obtained here. The 2008 cyclone (Fig. 4c – left panel) had been formed over the south of Argentina and propagated to ENE up to approximately 45°S x 20°W, where it had remained for some days while deepening. This event presented the lowest modeled SWH, 1.86-m (Fig. 4c – right panel). This value occurred 2.85-day after the waves had left the generation zone, as already mentioned in section 4. The cyclone responsible for the 2009 event (Fig. 4d – left panel) had been formed over the east of Uruguay and propagated to ESE up to approximately 42°S x 33°W. At this position, the cyclone deepened for 1.5-day and generated waves up to 2.95-m (Fig. 4d – right panel). The 2008 and 2009 cyclones had remained at higher latitudes compared to the others (1988, 1997 and 2010) at the moment they generated waves toward GB. The highest modeled SWH (4.68-m) (Fig. 4e – right panel) was produced by the 2010 cyclone (Fig. 4e – left panel), which had been formed over the southern coast of Brazil, as well as the 1997 cyclone. A remarkable atmospheric trough was presented in low levels before the cyclone formation. Then, after had been formed, the cyclone moved southeastward and remained close to GB. The region of formation and the trajectory of the 2010 cyclone were very similar to those of the 1997 cyclone. Additionally, due to the proximity of the coast, both 1997 and 2010 cyclones presented short wave fetches.

In general, it could be observed that SSE was

the predominant peak wave direction in times of maxims SWHs. Unlike the others, the peak wave direction of the 1988 event presented the value of 179° (S) in the instant of maximum SWH (Fig. 4a – right panel). However, this parameter changed its direction from S to SSE in subsequent times. Similar characteristics occurred with DPs in the 1997 and 2010 events (Figs. 4b and 4e – right panels). Both 2008 and 2009 events exhibited more stable values of about 160° (SSE) for the peak wave direction parameter around the times of maximum SWH (Figs. 4c and 4d – right panels).

Peak wave periods ranged from 11.66 to 13.39-s in times of maxims SWHs. The highest modeled TP (15.06-s) occurred in the 2008 event, 62-h before the time of maximum SWH. The lowest TPs were produced by the 1997 and 2010 events, 11.66 and 12.66-s respectively (Figs. 4b and 4e – right panels). These relatively low values of TP can be attributed to short wave fetches, resulting from the proximity of the cyclones to the mouth of GB. The cyclone responsible for the 1988 event, which had moved a little farther south than the cyclones of 1997 and 2010, generated waves with TP of 13.35-s (Fig. 4a – right panel) in the time of maximum SWH. This value is on the same order of magnitude of the TP values of the 2008 and 2009 events, which were 13.39 and 13.16-s respectively (Figs. 4c and 4d – right panels). The waves generated by the 1988, 2008 and 2009 cyclones had not been limited by short wave fetches.

A digest of modeled mean wave parameters values in times of maxims SWHs can be found in Table II.

Table II. Modeled mean wave parameters values in times of maxims significant wave heights.

| Date of the event | Significant wave height (m) | Peak wave direction (deg.) | Peak wave period (s) |
|-------------------|-----------------------------|----------------------------|----------------------|
| 11/08/1988 | 4.37 | 179.0 | 13.35 |
| 31/05/1997 | 3.85 | 165.3 | 11.66 |
| 24/04/2008 | 1.86 | 152.8 | 13.39 |
| 02/10/2009 | 2.95 | 162.6 | 13.16 |
| 08/04/2010 | 4.68 | 160.0 | 12.66 |
| Mean | 3.54 | 163.9 | 12.84 |

Table III shows a statistical comparison between EHSW and NWW3 simulated time series of SWH, TP and DP at the NWW3P. The time range of NWW3 results does not include the 1988 and 2010

events. Hence, the 1997, 2008 and 2009 events were selected to perform the wave statistics. Figure 5 (Appendix) shows the time series corresponding to the statistical values depicted in Table III.

Table III. Comparison statistics for significant wave height (SWH), peak wave period (TP) and peak wave direction (DP) time series hindcasted by EHSW and NWW3 simulations for the years of 1997, 2008 and 2009 at the NWW3P (42.5°W x 23°S). Std, RMSE, SI and R stand for standard deviation, root-mean-square error, scatter index and correlation coefficient, respectively. The Bias and RMSE statistical indices are in meters, seconds and degrees for SWH, TP and DP, respectively. The time series corresponding to the statistical values depicted in this table can be seen in Figure 5 of the Appendix.

| Event - Parameter | Mean NWW3 | Std NWW3 | Mean EHSW | Bias | RMSE | SI | R |
|-------------------|-----------|----------|-----------|-------|-------|------|------|
| 1997 - SWH | 3.35 | 1.23 | 2.81 | -0.54 | 0.64 | 0.19 | 0.96 |
| 2008 - SWH | 1.78 | 0.27 | 1.37 | -0.41 | 0.43 | 0.24 | 0.86 |
| 2009 - SWH | 2.46 | 0.60 | 2.11 | -0.35 | 0.49 | 0.19 | 0.82 |
| 1997 - TP | 11.31 | 1.49 | 10.84 | -0.46 | 1.10 | 0.09 | 0.74 |
| 2008 - TP | 11.48 | 2.15 | 12.09 | 0.61 | 2.56 | 0.22 | 0.15 |
| 2009 - TP | 10.94 | 1.09 | 11.12 | 0.18 | 1.13 | 0.10 | 0.63 |
| 1997 - DP | 172.45 | 18.86 | 178.24 | 5.78 | 15.42 | 0.08 | 0.68 |
| 2008 - DP | 159.99 | 24.89 | 175.00 | 15.01 | 34.84 | 0.21 | 0.01 |
| 2009 - DP | 161.03 | 13.58 | 159.63 | -1.39 | 13.80 | 0.08 | 0.65 |

Regarding the SWH parameter, the bias values indicate that the three EHSW results underestimated the NWW3 results. A further investigation would be necessary for assessing the trade-off between the spatial resolutions of the wave and wind fields of both hindcasts (EHSW and NWW3), since the EHSW simulations have a better/worse spatial resolution of the wave/wind fields than the NWW3 simulation. In this case, the wave/wind fields of the EHSW simulations have a spatial resolution that is 60-times finer/~1.5-times coarser than the NWW3 simulation. It would be a pertinent discussion for a future study, especially in shallow waters, in which several runs should be carried out with different settings of spatial resolution for wave and wind fields to determine the prevailing element in the SWH results. However, it is out of the scope of this work and for the purpose of comparison, we assume here the mean wave parameters are truly represented by the NWW3 results. Despite of underestimations, the shapes of the SWH curves (Fig. 5 - Appendix) are generally similar in both hindcasts for the three events, with minor differences at specific times. This can be noted by the high correlation coefficient values for SWH. An analogous pattern occurs for the correlation coefficient values for DP and TP in the 1997 and 2009 events. It is interesting to note the extremely low correlation coefficient values for DP and TP in the 2008 event. The differences between the NWW3 (black circles) and EHSW (red circles) simulated TP curves (Fig. 5 - Appendix) in the 2008 event is more evident than between the curves of DP. The first seems to be more

associated with a time lag, while the second has a 90-degree discrepancy for approximately one day, which represents 14 % of the time series.

In general, the scatter index values were relatively low for all mean wave parameters in the three events. The highest SI values were found in the 2008 event, SI = 0.24, SI = 0.22 and SI = 0.21 for SWH, TP and DP, respectively. The highest RMSE values for TP and DP were also found in the 2008 event (RMSE = 2.56 and RMSE = 34.84, respectively), while the highest RMSE value for SWH (RMSE = 0.64) was noticed in the 1997 event. Regarding the mean values, the highest differences between EHSW and NWW3 simulations were all found in the 2008 event, with underestimation of 23 % for SWH and overestimations of 5 % for TP and 9 % for DP. On the other hand, the highest standard deviation (Std) values for TP and DP of the NWW3 simulation were also found in the 2008 event, and from their ranges, the mean values of the EHSW simulations for these parameters would suit the mean values of NWW3 simulation.

Three of the five EHSW happened in autumn (1997, 2008 and 2010), one in winter (1988) and one in spring (2009). A conclusion on the seasonal preference of EHSW cannot be drawn, since this set of events consists of a very restricted sample set. On the other hand, the table of monthly and seasonal climatologies created for the NWW3P (Table IV) shows that the winter months (June, July and August - JJA) present the highest mean seasonal value of SWH, followed by spring (September, October, November -

SON), autumn (March, April, May - MAM) and summer (December, January, February - DJF), respectively. These results are in accordance with the study of Gan & Rao (1991) for winter and summer seasons, in which the authors observed that the frequency of cyclogenesis is more in winter and less in summer than in any other season. Although, in transition seasons, the frequency of cyclogenesis is more in autumn than in spring. The results for winter also reinforce the work of Young (1999), which showed that winter is the season with the roughest wave conditions in both hemispheres. Observing month-by-month (Table IV), the highest mean wave heights are found in months of transition seasons. In Table IV, one can note that September is the month with the highest mean SWH (1.81-m), followed by May (1.79-m). However, the wave heights vary more in May than in September, which can be inferred from the standard deviation values (Std). Lemos & Calbete (1996) assessed a 9-year (1987-1995) period of satellite imagery and synoptic charts, concluding that September is the second month with the highest number of cold fronts that move along the Brazilian shore. Thus, the same cyclones associated with this great number (6) of cold fronts are probably associated with the highest mean SWH. The second highest mean

SWH can be explained by the high frequency of cyclogenesis in May (Gan & Rao, 1991). Higher wave heights occur in the presence of cyclonic systems and lower wave heights in their absence. This fluctuation between big and small waves leads to a high Std value in May.

Regarding the peak wave period monthly climatology, the highest value is found in May (9.83-s), followed by the winter months, and the lowest value is found in January (7.74-s). In the seasonal climatology, winter shows the highest TP (9.5-s), followed by autumn, spring and summer, respectively (Table IV).

In terms of peak wave direction, the monthly climatological values for the NWW3P (Table IV) vary in the range of 120 and 162°. The highest value is found in May, suggesting a strong correspondence with the high frequency of cyclogenesis in this month. The standard deviation values vary from 32.7 to 45.9°, which indicate that waves coming from E to SSW can reach the NWW3P. Waves coming from other directions do not reach the NWW3P, which can be verified by looking at the coastline orientation (Fig. 1). According to the seasonal mean values of DP, the most energetic waves come from ESE in summer, from SE in spring and from SSE in the other seasons.

Table IV. Monthly and seasonal climatologies (1997-2009) of modeled mean wave parameters for the NWW3P.

| Months | Significant wave height (SWH) | | Peak wave period (TP) | | Peak wave direction (DP) | | Seasonal mean values of SWH, TP and DP |
|-----------|-------------------------------|---------|-----------------------|---------|--------------------------|------------|---|
| | Mean (m) | Std (m) | Mean (s) | Std (s) | Mean (deg.) | Std (deg.) | |
| January | 1.28 | 0.41 | 7.74 | 1.74 | 120.0 | 45.9 | Summer (DJF): 1.29-m; 7.95-s; 127.1° |
| February | 1.26 | 0.42 | 8.19 | 2.05 | 130.3 | 45.0 | |
| March | 1.34 | 0.47 | 8.64 | 2.09 | 140.7 | 38.6 | Autumn (MAM): 1.55-m; 9.26-s; 151.7° |
| April | 1.53 | 0.54 | 9.30 | 2.16 | 152.7 | 36.4 | |
| May | 1.79 | 0.61 | 9.83 | 1.92 | 161.7 | 32.7 | Winter (JJA): 1.67-m; 9.5-s; 147.6° |
| June | 1.61 | 0.65 | 9.71 | 2.04 | 152.8 | 41.0 | |
| July | 1.71 | 0.56 | 9.65 | 1.90 | 153.0 | 38.2 | Spring (SON): 1.65-m; 8.45-s; 132.1° |
| August | 1.69 | 0.53 | 9.14 | 2.00 | 137.0 | 43.6 | |
| September | 1.81 | 0.52 | 8.94 | 2.03 | 138.6 | 43.6 | |
| October | 1.58 | 0.46 | 8.20 | 1.71 | 128.7 | 40.7 | |
| November | 1.55 | 0.54 | 8.20 | 1.86 | 129.0 | 45.2 | |
| December | 1.34 | 0.45 | 7.93 | 1.80 | 131.0 | 45.3 | |

Final remarks

In this paper we have described five numerically hindcasted events of high sea waves at the mouth of Guanabara Bay corresponding to real EHSW reported by the media. For this purpose, wave hindcasts were carried out employing the WAVEWATCH III model forced by wind fields from the NCEP-NCAR Reanalysis I project. A validation of the EHSW simulations was carried out by comparing their results to the global wave hindcast results generated by the NOAA (NWW3) at the nearest NWW3 grid point, 23°S x 42.5°W. At this same point, monthly and seasonal climatologies of mean wave parameters were computed to estimate mean values close to the region of study.

Cyclones were the atmospheric systems responsible for generating the investigated EHSW, producing strong winds during their mature stages. The three cyclogenetic regions of South America, cited in the literature, have sufficient energy to generate strong cyclones, as exposed here. The region of cyclogenesis may play an important role in SWHs, which can be supported by the idea that two (1997 and 2010) of the three (1988, 1997 and 2010) events that produced the biggest waves were formed in the same region.

The highest and lowest significant wave heights were produced by the 2010 and 2008 events, respectively. Short wave fetches did not preclude high sea waves in the 1997 and 2010 events. The highest peak wave periods were associated with cyclones whose trajectories were farther South in relation to Guanabara Bay (1988, 2008 and 2009 events). The 1988 event was the only one which presented peak wave direction of S in the time of maximum SWH, while the others presented SSE. The mean wave parameters presented mean values of 3.54-m for SWH, 12.84-s for TP and 163.9° for DP in times of maxims SWHs.

It was not possible to verify the hindcasted results exactly at the mouth of Guanabara Bay. However, the model implemented here was able to closely match the mean wave parameters simulated by the NOAA global wave hindcast in the three simulated years (1997, 2008 and 2009) available for comparison. In general, the worst statistical results for SWH, TP and DP were found in the 2008 event. Despite of the underestimation of SWH during the 1997, 2008 and 2009 events, the shape of the curves presented a good agreement for all parameters in both hindcasts.

According to the monthly climatological

results, generated from the NOAA global wave hindcast for the nearest point to the Guanabara Bay entrance, September and May presented the highest SWH values. The highest peak wave period and peak wave direction were also found in May. A seasonal analysis showed that winter exhibits the highest values of SWH and TP. On the contrary, the lowest seasonal values were found in summer. In terms of peak wave direction, waves come from directions between SSE and ESE in all seasons.

Numerical wave models have shown increasingly usefulness, especially owing to their ability to provide results for a large area in a relatively short period of time. They have become more and more precise and have been applied to hindcast significant events, forecast wave conditions and generate wave climatologies, implying more safety to the coastal and offshore engineering works. The results obtained here allow us to understand the order of magnitude of EHSW at the mouth of GB. This environment still needs to be more explored in terms of surface gravity waves and their impacts in the estuary given its economic and social importance. Other EHSW should be analyzed in order to better comprehend their relationship with climatology. Additionally, further studies need to be conducted concerning the atmospheric triggers that generate the cyclones responsible for EHSW.

Acknowledgements

The authors are thankful to Conselho Nacional de Desenvolvimento Científico e Tecnológico (CNPq - Process number 130060/2010-0) for funding the first author. We also would like to thank NOAA for providing the data used in this research and the two referees for comments that led to major improvements on the earlier version of this manuscript. Finally, we thank F. F. Ostritz and R. M. Campos for great advices in numerical modeling.

References

- Alves, J. H. G. M., Ribeiro, E. O., Grossmann Matheson, G. S., Lima, J. A. M. & Parente Ribeiro, C. E. 2009. Reconstituição do clima de ondas no sul-sudeste brasileiro entre 1997 e 2005. **Revista Brasileira de Geofísica**, 27(3): 427-445.
- Amante, C. & Eakins, B. W. 2009. ETOPO1 1 arc-minute global relief model: procedures, data sources and analysis. **NOAA Technical Memorandum NESDIS NGDC-24**, Boulder,

- Colorado, 19 p.
- Beu, C. M. L. & Ambrizzi, T. 2006. Variabilidade interanual e intersazonal da frequência de ciclones no Hemisfério Sul. **Rev. Brasileira de Meteorologia**, 21(1): 44-55.
- Candella, R. N., Grossmann, G. S. & Quental, S. H. A. 1999. Reconstituição de condições de ondas no oceano Atlântico Sul com a utilização de modelo de terceira geração. **Pesquisa Naval**, 12: 23-34.
- Cavaleri, L. & Malanotte-Rizzoli, P. 1981. Wind-wave prediction in shallow water: Theory and applications. **Journal of Geophysical Research**, 86: 961-973.
- Chawla, A., Spindler, D. M. & Tolman, H. L. 2013. Validation of a thirty year wave hindcast using the Climate Forecast System Reanalysis winds. **Ocean Modelling**, 70: 189-206.
- CIDS – Centro Internacional de Desenvolvimento Sustentável; Baía de Guanabara Dossiê Sócio-Ambiental, Rio de Janeiro, Brazil, 2000.
- Dragani, W. C., Cerne, B. S., Campetella, C. M., Possia, N. E. & Campos, M. I. 2013. Synoptic patterns associated with the highest wind-waves at the mouth of the Río de la Plata estuary. **Dynamics of Atmospheres and Oceans**, 61-62: 1-13.
- Gan, M. A. & Rao, V. B. 1991. Surface cyclogenesis over South America. **Mon. Wea. Rev.**, 119: 1293-1302.
- Hasselmann, K., Barnett, T. P., Bouws, E., Carlson, H., Cartwright, D. E., Enke, K., Ewing, J. A., Gienapp, H., Hasselmann, D. E., Kruseman, P., Meerburg, A., Mueller, P., Olbers, D. J., Richter, K., Sell, W. & Walden, H. 1973. Measurements of wind-wave growth and swell decay during the Joint North Sea Wave Project (JONSWAP). **Ergänzungsheft zur Deutschen Hydrographischen Zeitschrift**, Reihe A(8°), 12, 95 p.
- Hasselmann, S., Hasselmann, K., Allender, J. H., & Barnett, T. P. 1985. Computations and parameterizations of the nonlinear energy transfer in a gravity-wave spectrum, Part II: parameterizations of the nonlinear energy transfer for application in wave models. **Journal of Physical Oceanography**, 15: 1378-1391.
- Holliday, N. P., Yelland, M. J., Pascal, R., Swail, V. R., Taylor, P. K., Griffiths, C. R. & Kent, E. 2006. Were extreme waves in the Rockall Trough the largest ever recorded? **Geophys. Res. Lett.**, 33: L05613.
- Innocentini, V. & Caetano Neto, E. S. 1996. A case study of the 9 August 1988 South Atlantic storm: numerical simulations of the wave activity. **Weather and Forecasting**, 11: 78-88.
- Innocentini, V., Oliveira, F. A. & Prado, S. C. S. C. 2003. Modelo de ondas aplicado ao caso 5-8 de maio de 2001. **Rev. Brasileira de Meteorologia**, 18(1): 97-104.
- Kalnay, E., Kanamitsu, M., Kistler, R., Collins, W., Deaven, D., Gandin, L., Iredell, M., Saha, S., White, G., Woollen, J., Zhu, Y., Chelliah, M., Ebisuzaki, W., Higgins, W., Janowiak, J, Mo, K. C., Ropelewski, C., Wang, J., Leetmaa, A., Reynolds, R., Jenne, R. & Joseph, D. 1996. The NCEP/NCAR 40-year reanalysis project. **Bullet. Am. Meteorol. Soc.**, 77: 437-471.
- Khandekar, M. L. & Swail, V. R. 1995. Storm waves in Canadian waters: a major marine hazard. **Atmosphere-ocean**, 33(2): 329-357.
- Kjerfve, B., Ribeiro, C. H. A., Dias, G. T. M., Filippo, A. M. & Quaresma, V. S. 1997. Oceanographic characteristics of an impacted coastal bay: Baía de Guanabara, Rio de Janeiro, Brazil. **Continental Shelf Research**, 17(13): 1609-1643.
- Ledden, M. V., Vaughn, G., Lansen, J., Wiersma, F. & Amsterdam, M. 2009. Extreme wave event along the Guyana coastline in October 2005. **Continental Shelf Research**, 29: 352-361.
- Lemos, C. F. & Calbete, N. O. 1996. Sistemas frontais que atuaram no litoral de 1987 a 1995. **Climanálise – Boletim de monitoramento e análise climática – INPE/CPTEC**, Cap.14.
- Rocha, R. P., Sugahara, S. & Silveira, R. B. 2004. Sea waves generated by Extratropical cyclones in the South Atlantic Ocean: hindcast and validation against altimeter data. **Weather and forecasting**, 19: 398-410.
- Reboita, M. S., Rocha, R. P., Ambrizzi, T. & Sugahara, S. 2010. South Atlantic Ocean cyclogenesis climatology simulated by regional climate model (RegCM3). **Clim. Dyn.**, 35: 1331-1347.
- Satyamurty, P., Ferreira, C. C. & Gan, M. A. 1990. Cyclonic vortices over South America. **Tellus**, 42A: 194-201.
- Seluchi, M. E. 1995. Diagnóstico y pronóstico de situaciones sinópticas conducentes a ciclogénesis sobre el este de Sudamérica. **Geofísica Internacional**, 34(2): 171-186.

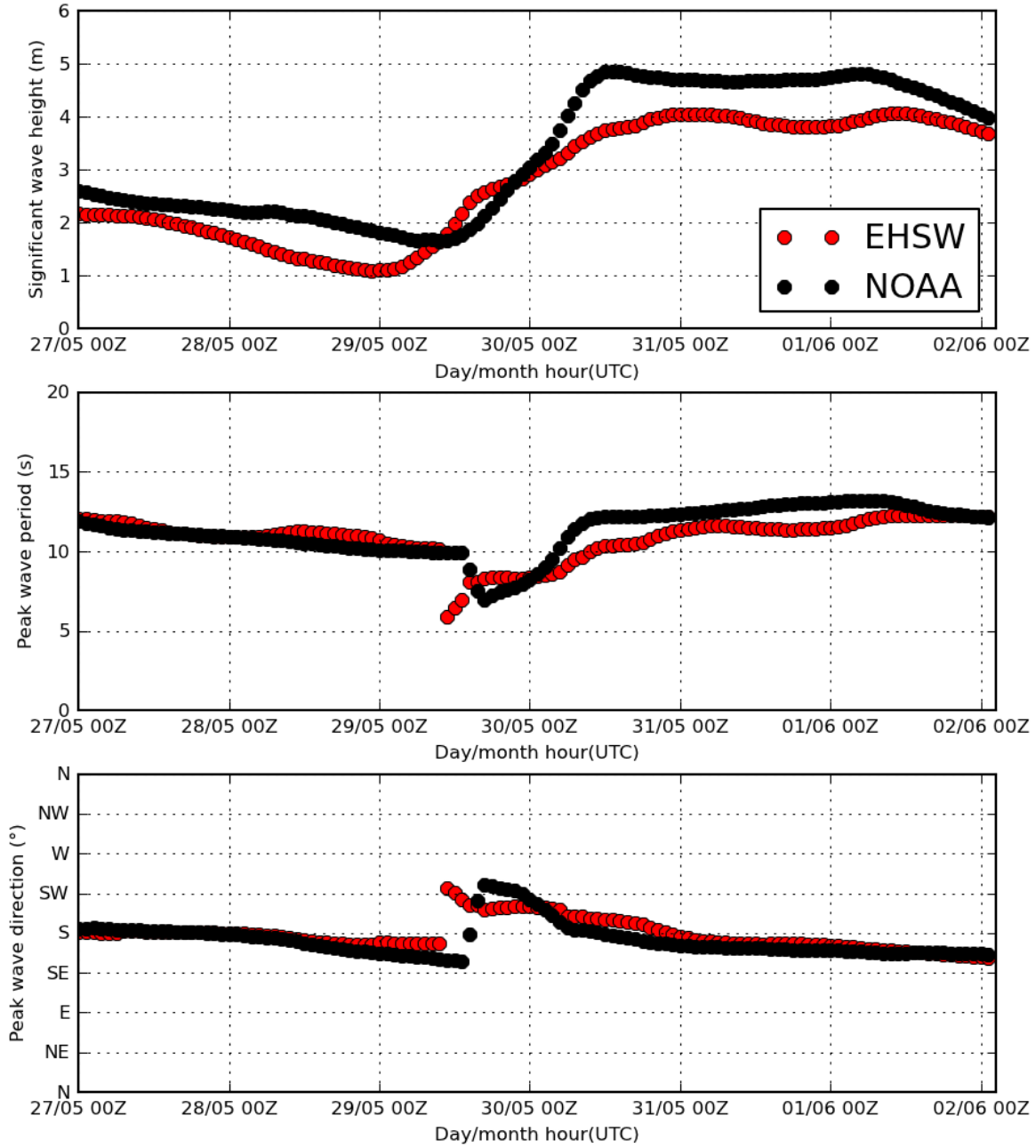
- Sinclair, M. R. 1995. A climatology of cyclogenesis for the Southern Hemisphere. **Mon. Wea. Rev.**, 123: 1601-1619.
- Stephens, S. A. & Gorman, R. M. 2006. Extreme wave predictions around New Zealand from hindcast data. **New Zealand Journal of Marine and Freshwater Research**, 40: 399-411.
- Stopa, J. E., Cheung, K. F. & Chen, Y. 2011. Assessment of wave energy resources in Hawaii. **Renewable Energy**, 36: 554-567.
- Streten, N. A. & Troup, A. J. 1973. A synoptic climatology of satellite observed cloud vortices over the Southern Hemisphere. **Quart J. R. Met. Soc.**, 99: 56-72.
- Tolman, H. L. 2009. User Manual and System Documentation of WAVEWATCH III version 3.14. **NOAA/ NWS/ NCEP/ MMAB Technical Note 276**, 194 pp + Appendices.
- Tolman, H. L. & Chalikov, D. V. 1996. Source terms in a third-generation wind-wave model. **Journal of Physical Oceanography**, 26: 2497-2518.
- Young, I. R. 1999. Seasonal variability of the global ocean wind and wave climate. **International Journal of Climatology**, 19: 931-950.

Received February 2014

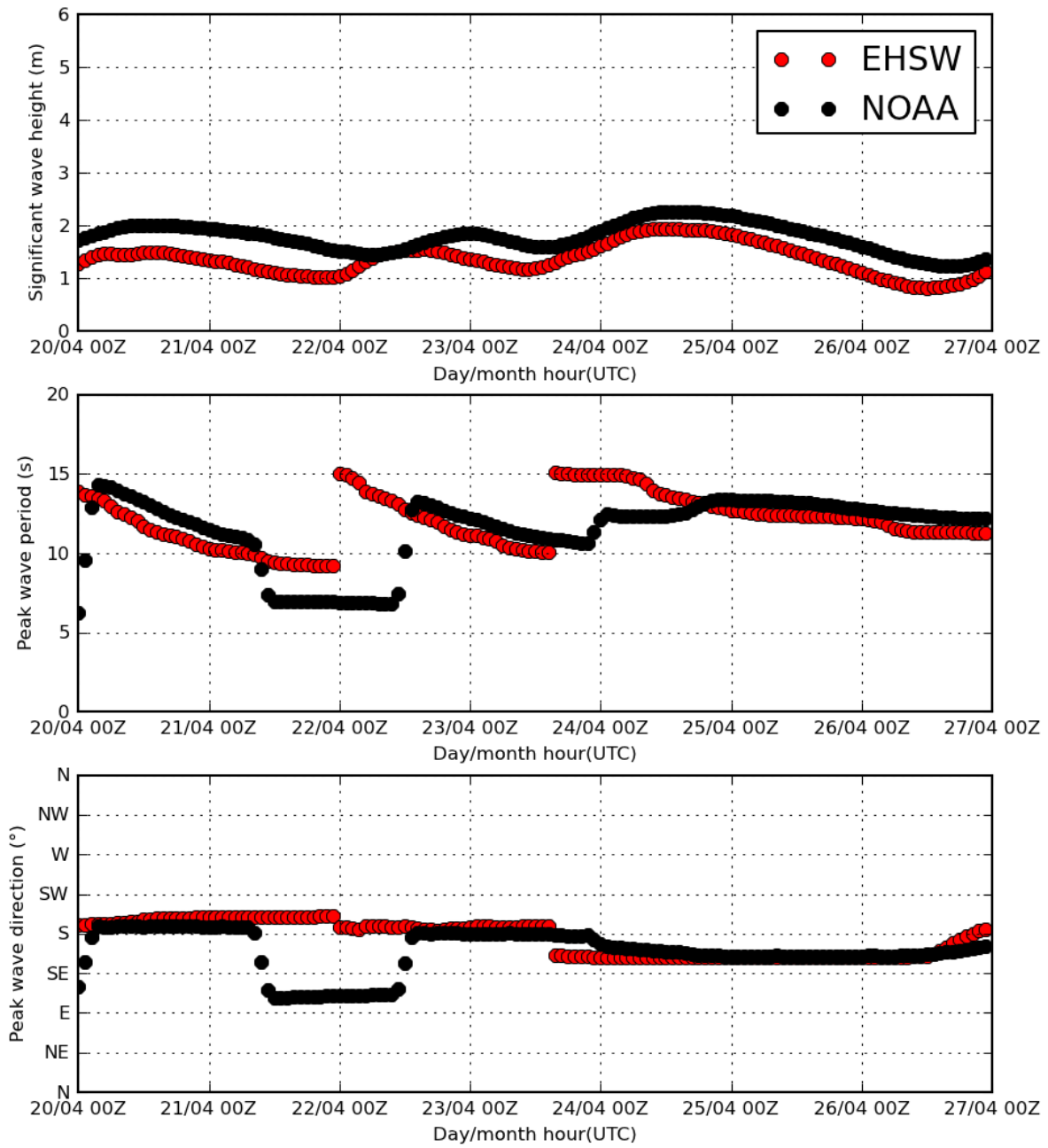
Accepted June 2014

Published online August 2014

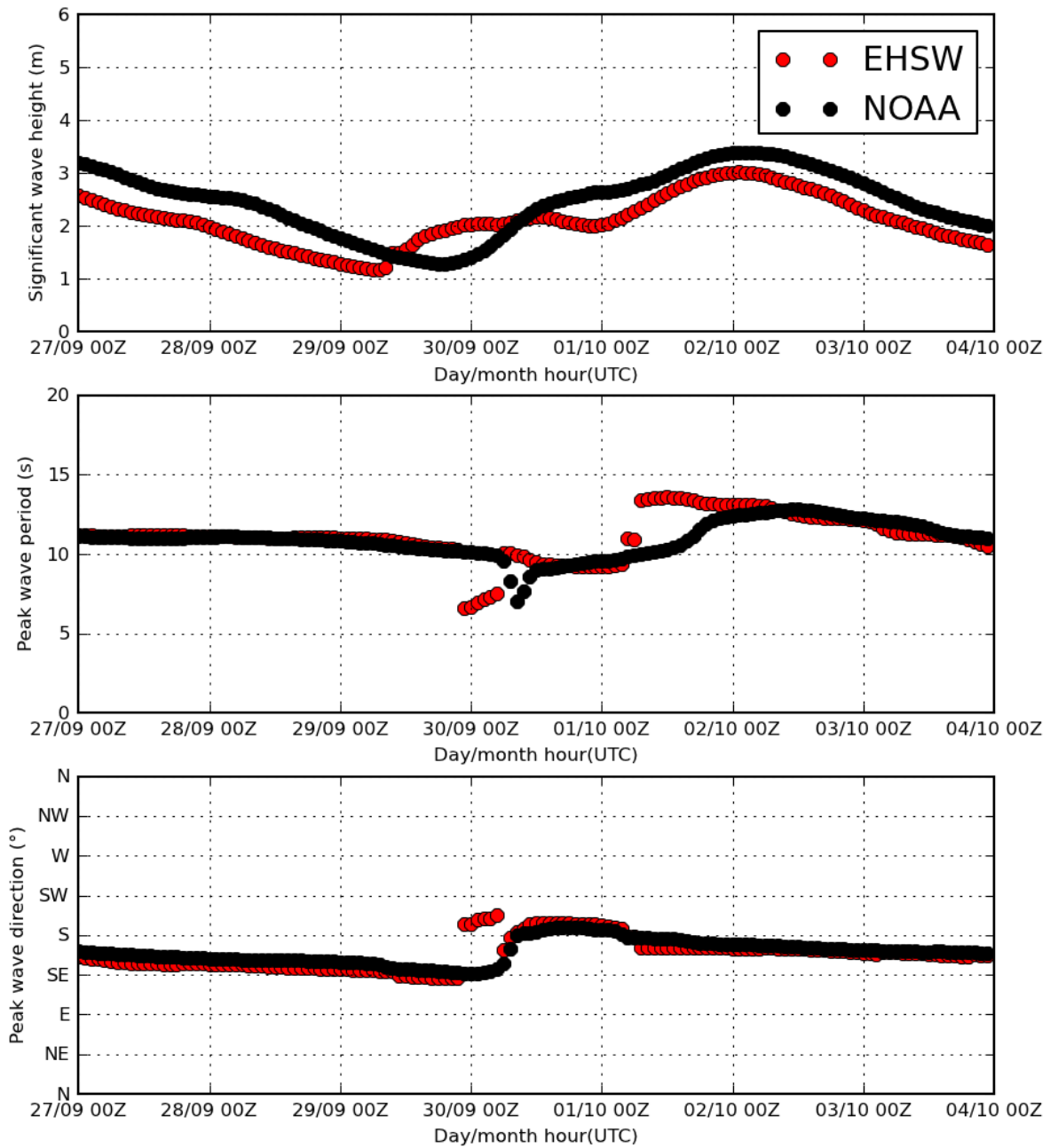
Appendix Time series corresponding to the statistical values shown in Table III.



(a)



(b)



(c)

Figure 5. Hindcasted time series of significant wave height (upper panel), peak wave period (middle panel) and peak wave direction (lower panel) for the years of (a) 1997; (b) 2008; (c) 2009. The black and red circles represent the NWW3 (carried out by the NOAA) and EHSW simulated values, respectively.